THE MAGNETISATION PROCESS IN A TWO–PHASE EXCHANGE–COUPLED SYSTEM: A MICROSCOPIC STUDY

D. H. Ryan,
Physics Department, McGill University, 3600 University St., Montreal, Quebec H3A 2T8, Canada
E.H. Feutrill and J. Ding,
Department of Physics, The University of Western Australia, Nedlands, Australia 6097

Abstract

The magnetisation process in an exchange-coupled $\alpha-$Fe + $Nd_2Fe_{14}B$ nanocomposite has been studied by Mössbauer spectroscopy. Measurements in fields of up to 2 Tesla confirm that the magnetisation of the soft phase is strongly coupled to that of the hard phase. Analysis of magnetisation curves and magic-angle spectra of saturated samples shows that the remanence is dominated by the hard phase.

PACS numbers: 75.50.Ww 75.50.Bb 75.50.Tt 76.80.+y

Introduction

Nanocomposite magnets containing fine grained hard and soft magnetic phases in intimate contact have been shown to exhibit some unusual properties. Their remanence ratio (M_r/M_{sat}) can be as much as 0.7, well above the value of 0.5 expected for an isotropic uniaxial powder, and leading to the term "HIREM" being used to describe them [1]. They also show an unusual tendency to recover from the application of a reverse field, the magnetisation 'springs' back almost to its original value even after the application of a reverse field large enough to halve the magnetisation.

Normally, the presence of a soft magnetic impurity in a hard magnet leads to a degradation of performance as the soft phase provides easy nucleation sites for magnetisation reversal. However, if the hard and soft grains are small enough (typically less than the thickness of a domain wall) then is no longer possible to start a reversal in the soft phase and the magnetisations of the two phases are locked together [2]. In an optimised sample, the soft phase (*e.g.* $\alpha-$Fe) has a high magnetisation and provides the saturation magnetisation, while the hard phase (*e.g.* $Nd_2Fe_{14}B$) provides the resistance to reversal. This is the mesoscopic analogue of most hard magnet alloys, where the rare-earth provides anisotropy and iron provides magnetisation.

Several numerical models have been developed to describe the magnetisation process in an exchange-coupled magnet [3] and they lead to the following results: Although an isotropic powder of a hard phase can yield a remanence ratio of no more than 0.5 by having the magnetisation of each grain oriented within the upper hemisphere (*i.e.* never worse that perpendicular to the bulk magnetisation), the soft phase in which it is dispersed responds to the average of several neighbouring hard grains and tends, on average, to have its local magnetisation closer to the bulk direction and so contributes more than 0.5 of its M_{sat}. When a reverse field is applied, the initial response is primarily in the soft phase with little effect on the hard grains, so that after the field is removed, the magnetisation of the soft phase returns to its initial value as the hard grains, which define the zero-field magnetisation of the soft phase, are still in their original orientations.

While the agreement between microscopic models and bulk behaviour is quite good, we felt it would be appropriate to test the models at a microscopic level. To this end we set out to follow the rotation of the magnetisation in an exchange-coupled system by Mössbauer spectroscopy. This technique allows us to see the magnetisation direction through the intensities of lines 2 and 5 of the magnetically split 6-line spectrum. Furthermore, if the spectra of the two magnetic phases are sufficiently well separated, we can monitor the magnetisation direction in each phase independently. We report here on an exchange coupled $\alpha-$Fe + $Nd_2Fe_{14}B$ nanocomposite, chosen because of the complete separation of lines 5 and 6 in this combination and also because the Mössbauer spectra of both components have been extensively studied and excellent fits are available.

Experimental Methods

An arc-melted ingot of $Nd_{10}Fe_{85}B_5$ was crushed and ball-milled under argon for 20 hours in a SPEX 8000 mixer-mill. the resulting amorphous powder was then crystallised by annealing at 600 °C for 30 minutes. Mössbauer spectroscopy and thermogravimetric analysis (TGA) in a small field gradient confirmed that the only phases present were: $\alpha-$Fe ($\sim$ 27% by weight) $Nd_2Fe_{14}B$ ($\sim$ 68%) with the balance being $Nd_{1.1}Fe_4B_4$. The sample for applied-field Mössbauer was prepared by mixing the annealed powder with epoxy to form a disc 16mm in diameter and 2mm thick. A piece of this was used for magnetisation measurements. Despite the high concentration of a magnetically soft phase, the hysteresis loop showed conventional single magnetic phase behaviour, and demagnetisation curves measured following saturation (Fig. 1) show magnetisation recovery typical of an exchange-spring system. A remanence of 103 J/T/kg was observed at zero internal field (a field of 0.4 T was used to cancel demagnetising field of the sample, determined from fits to the Mössbauer spectra). This is 60% of the expected saturation value calculated from the phase composition, demonstrating that the sample exhibits significantly enhanced remanence.

Mössbauer measurements were carried out at room temperature on a conventional constant acceleration spectrometer. A field of up to 2.2 Tesla was applied perpendicular to the $\gamma-$beam using a Harvey-Wells electromagnet. The 1GBq ^{57}Co**Rh** source was located well out of the pole gap so that stray fields at the source never exceeded 100mT. The sample was initially magnetised perpendicular to the disc surface in 2.2T and then spectra were recorded with the field applied parallel to the disc surface to observe the rotation of the magnetisation. Spectra were fitted using a conventional non-linear least-squares minimisation routine with the hyperfine parameters of all three phases fixed to values determined from standards [4]. The adjustable parameters were: baseline, linewidth, relative proportions of each phase, intensity of lines 2 and 5 (R) for each of the two magnetic phases and a field shift to include the effect of the externally applied field. Typical spectra are shown in Fig. 2.

Results and Discussion

The demagnetisation curves in Fig. 1 show that the remanent magnetisation largely recovers for reverse external fields of up to 0.4T but is rapidly destroyed in larger fields, with 0.55T being sufficient to reduce the remanence to zero. A field of 1.6T is sufficient to close the hysteresis loop. These curves set the scale for the expected changes in the Mössbauer spectra.

Inspection of the spectra in Fig. 2 show that the combination of $\alpha-$Fe and $Nd_2Fe_{14}B$ is ideally suited to the study of magnetisation rotation in an exchange-spring system as lines 5 and 6 for each phase are clearly separated. In each case, the right-hand component of the doublets centred at 3 mm/s and 5 mm/s belongs to $\alpha-$Fe while the left-hand component is due to $Nd_2Fe_{14}B$. Fig. 3 shows the fitted intensities of lines 2 and 5 (R) for the two magnetic components in the sample for various fields with data from a pure iron foil for comparison. The behaviour of the pure foil is as expected, with the remanent field of 0.6mT in the electromagnet being nearly enough to saturate the magnetisation. The maximum value of 3.6 (less than the theoretical value of 4.0) was limited by absorption saturation effects in the rather thick foil used.

The behaviour of the exchange-spring system is less easily accounted for. R_{Fe} responds much more slowly than in the pure foil, strong evidence that it is indeed exchange coupled to the hard phase. It also saturates in about 1.5 Tesla, consistent with the magnetisation curve in Fig. 1. The rather low saturation value of $\sim$3.2 is due in part to absorption saturation effects, but exchange coupling to the hard phase also restricts the degree to which the iron moments can orient parallel to the external field. By contrast, R_{2-14-1} increases quite slowly with the field, rising linearly with no sign of saturation, even in fields where the magnetisation curve (Fig. 1) has clearly flattened. If the trend continues, then a field of $\sim$3.5T would be needed before R_{2-14-1} would meet R_{Fe}. The recoil response is perhaps more surprising. The open points to the left of zero in Fig. 3 show results obtained in zero field after the sample had been exposed to external fields of 1.5T and 2.0T and in both cases the sample appears to return to its initial state, even though the magnetisation curve shows a substantial remanence. The small change apparent in Fig. 3 is close to the fitting uncertainty.

The apparent contradiction between the Mössbauer and magnetisation data is easily resolved when the structure of the sample is taken into account. Dispersing a ball-milled powder of an easy-axis magnet, such as $Nd_2Fe_{14}B$, in epoxy should yield a crystallograpically isotropic sample, *i.e.* one with no preferred axis or direction and an as-cast, unmagnetised, sample will contain a uniform distribution of magnetisation directions. Since the intensities of lines 2 and 5 are given by: $R = (4\sin^2\theta)/(1+\cos^2\theta)$, we obtain R = 2.0. In the fully magnetised remanent state, the moments are distributed uniformly over a hemisphere giving a remanence ratio of 0.5 and R is still 2. If we now apply a reverse field to the sample, the magnetisation within each grain will tend to tip, however, in an easy axis system, the only way a significant change in magnetisation can occur is through a 180° flip which takes the magnetisation from largely anti-parallel to largely parallel to the applied field. This type of flip has no effect on the Mössbauer spectrum. R is a function of $\sin^2\theta$ and $\cos^2\theta$ only and so a flip from θ to $\theta+180°$ leaves R unchanged. As the magnetisation of an isotropic powder is reversed through a series of 180° flips, R remains equal to 2. Thus, in zero field, R is always independent of the state of magnetisation of any isotropic powder of an easy axis material. The slow, linear increase in R apparent in Fig. 3 is due to the magnetisation within grains canting away from the easy axis against the anisotropy field, in response to the applied field.

In order to check our interpretation, we made a series of 'magic angle' [6] measurements on the sample magnetised both parallel and perpendicular to the disc surface. We found R_{2-14-1} to be independent of both orientation and magnetisation state, as expected for an isotropic powder of an easy-axis system. Furthermore, the constant value of 2.26 ± 0.01 obtained suggests that the offset from 2.0 aparent in Fig. 3 is due to saturation effects, probably due to the presence of large agglomerates. An anisotropic magnetisation distribution would show up as an orientation dependence in R, while saturation due to a uniform thick sample would lead to an increase in R when the sample was tilted through 54.7°. Large spherical agglomerates appear the same thickness in all orientations, and no change in saturation occurs in any orientation. The soft phase showed a systematic anisotropic response consistent with some polarisation of the moments, however the effect was small, and close to the statistical uncertainty of the fits.

In conclusion, we have shown that the magnetisation of the soft $\alpha-$Fe phase is locked to that of the hard $Nd_2Fe_{14}B$ phase and a substantial field is needed to change its orientation. The angular dependence of R coupled with the magnetisation process in an isotropic powder of a uni-axial magnet precludes observation of the orientation of the magnetisation in the hard phase. While it is likely that the majority of the remanence enhancement in a spring magnet is due to polarisation of the soft phase, it is not possible to rule out some polarisation of the hard phase from Mössbauer data as previously claimed [5].

Acknowledgments

This work was supported by grants from the Natural Sciences and Engineering Research Council of Canada and Fonds pour la formation de chercheurs et l'aide à la recherche, Québec. We gratefully acknowledge technical assistance from F. van Gils with both the applied field measeurements and the design of the magic angle system.

Figure captions

Figure 1 Demagnetisation curves normalised to the magnetisation in 1.6 T, for the exchange-coupled sample studied here, showing single magnetic phase response despite the 27 wt.% of $\alpha-$Fe present. The inset shows the loss of remanence in zero field after exposure to increasing reverse fields. Note that little irreversible loss occurs for reverse fields of less than 0.4 T.

Figure 2 Mössbauer spectra for a sample initially magnetised parallel to the $\gamma-$beam, exposed to increasing fields perpendicular to the beam. The bottom spectrum was taken in zero field after measuring in 2.0 T. Note the clear separation of $\alpha-$Fe from $Nd_2Fe_{14}B$ in lines 5 and 6 of the spectra, in each case, the high velocity component of the doublet is due to $\alpha-$Fe.

Figure 3 Fitted intensities of lines 2 and 5 relative to 3 and 4 for the two phases in the sample. The response of a pure iron foil is shown as open triangles for comparison. The two pairs of open symbols plotted to the left of zero field show results obtained in zero field after the sample had been measured in 1.5T and 2.0T.

References

1. R.W. McCallum, A.M. Kadin, G.B. Clemente and J.E. Keem, J. Appl. Phys. **61** (1987), 3577–9. G.B. Clemente, J.E. Keem and J.P. Bradley, J. Appl. Phys. **64** (1988), 5299–5301.

2. E.F. Kneller and R. Harwig, IEEE Trans. Mag. **27** (1991), 3588–3600.

3. E.H. Feutrill, P.G. McCormick and R. Street, J. Appl. Phys. **75** (1994), 5701–3; T. Schrefl, J. Fidler and H. Kronmüller, Phys. Rev. **B49** (1994), 6100–10; R. Fischer, T. Schrefl, H. Kronmüller and J. Fidler, J. Magn. Magn. Mater **153** (1996), 35–49.

4. D.H. Ryan, Z. Altounian, J.O. Ström-Olsen and W.B. Muir, Phys. Rev. **B39** (1989), 4730–2.

5. J. Ding, R. Street and P.G. McCormick, J. Magn. Magn. Mater **140–4** (1995), 1071–2.

6. J.M. Greneche and F. Varret, J. Phys. C **15** (1982), 5333–44.

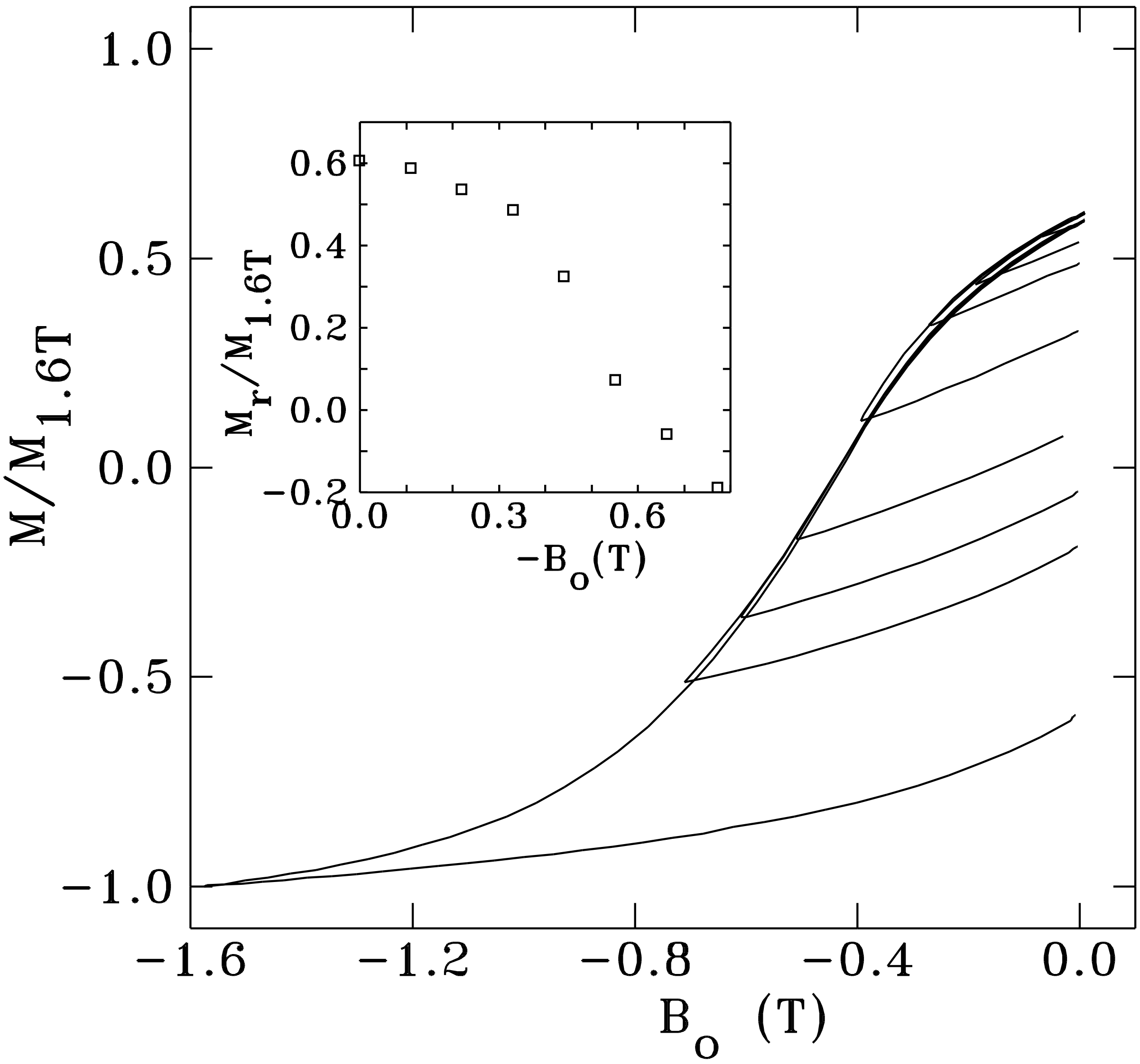

Figure 1: Ryan, Feutrill and Ding, MMM96 CE–02

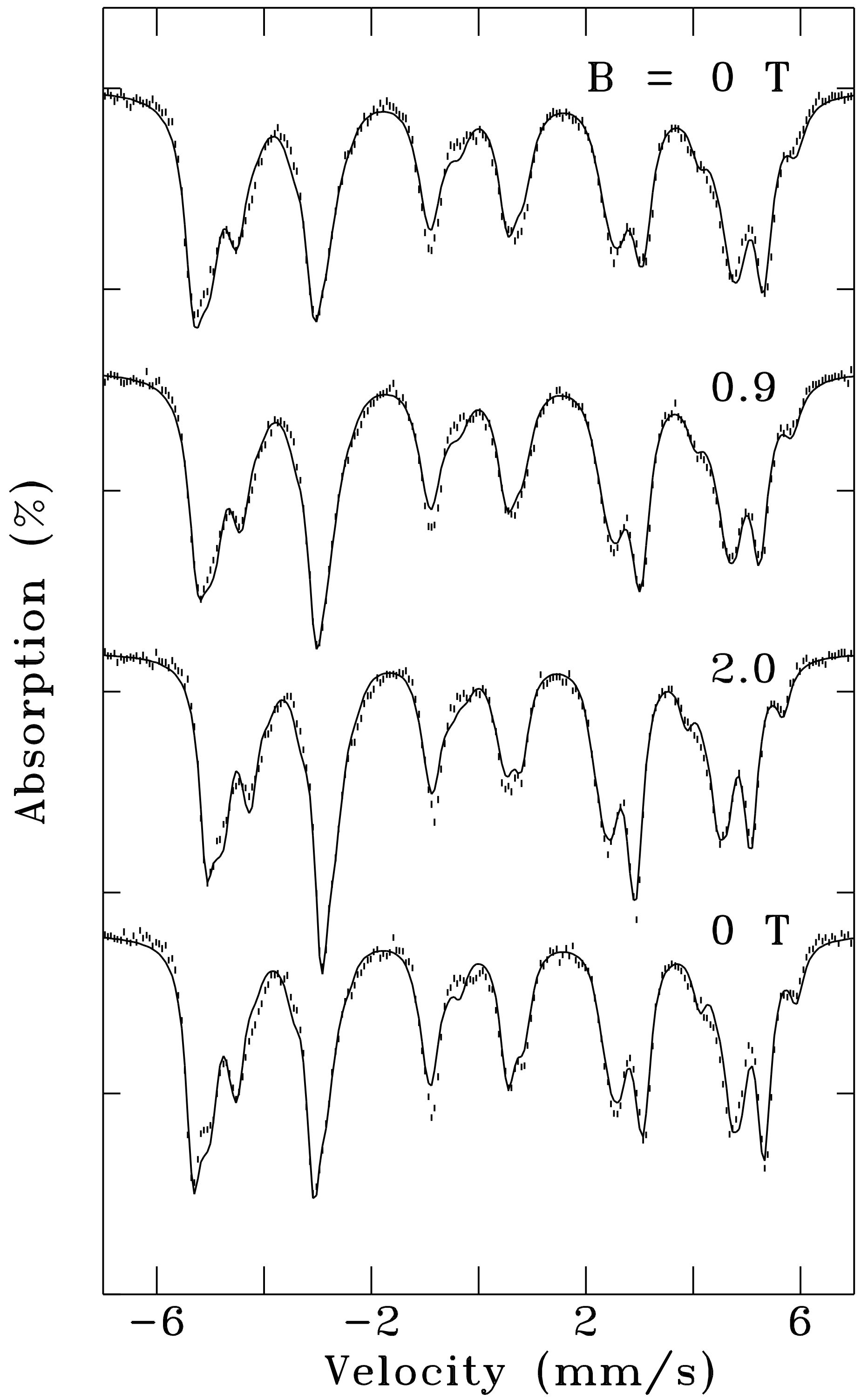

Figure 2: Ryan, Feutrill and Ding, MMM96 CE–02

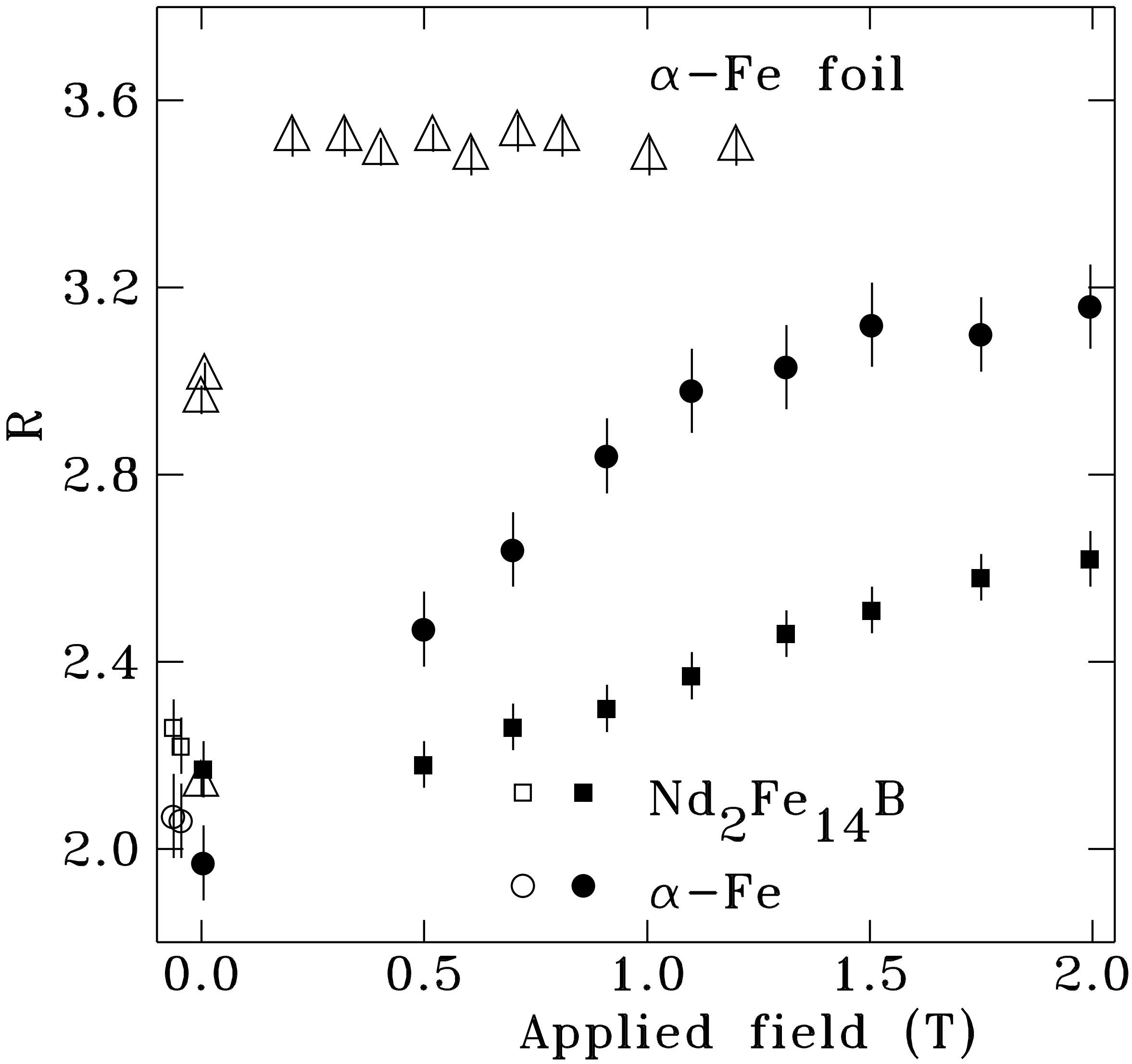

Figure 3: Ryan, Feutrill and Ding, MMM96 CE–02